# The Synthesis of Dimethyl Carbonate by the Oxicarbonylation of Methanol Over Cu Supported on Carbon Norit

**G. Merza · B. László · A. Oszkó · G. Pótári ·
E. Varga · A. Erdőhelyi**

**Abstract** The catalytic activity of Norit supported Cu, Ni and Cu–Ni catalysts was investigated in the synthesis of dimethyl carbonate (DMC) by the oxidative carbonylation of methanol. Cu/Norit showed the best catalytic activity. The reaction was carried out in a continuous flow system at atmospheric pressure usually at 393 K. The main products were methyl formate, DMC and $CO_2$. The methanol conversion on Cu/Norit achieved in steady state was about 22 % and the DMC yield 13.2 %. Based on the XPS data we can establish that copper reduced to its metallic form during reduction but oxidized in the reaction mixture, and is mostly in the $Cu^+$ state, with some $Cu^{2+}$. It is possible that the DMC formation rate depends on the surface concentration of oxidized Cu and on the ratio of $Cu^+$ and $Cu^{2+}$. Based upon the IR measurements adsorbed DMC was found on the surface of the Cu/Norit catalyst during the catalytic reaction.

**Keywords** Oxidative carbonylation · Dimethyl carbonate · Active carbon · Supported Cu catalyst · Cu/Norit

## 1 Introduction

As an environmentally friendly compound dimethyl carbonate (DMC) has the potential to be used as a green industrial chemical. Its usage is facilitated by its low toxicity, high biodegradability and low persistence [1]. DMC can be used in industry mainly as a fuel additive [2], precursor for synthesis of carbonic acid derivatives, methylating agent [3], methyl sulphate exchanger [4], or an intermediate in the synthesis of polycarbonates and isocyanates [5], carbonylating agent [6], alkylating agent, polar solvent [7], component in the synthesis of polyurethane [8].

Proving the possibilities of the green usage of DMC, a new alternative route for the enzymatic coproduction of biodiesel and glycerol carbonate was investigated by Seong et al. [9] by the transesterification of soybean oil with DMC.

The traditional DMC synthesis used toxic and hazardous phosgene as reactant and suffered from several drawbacks [10]. Numerous developments have been published for the production of DMC including methanolysis of phosgene, ester exchange process, liquid phase methanol carbonylation and methylnitrite carbonylation and gas-phase oxidative carbonylation of methanol [11] although these processes use corrosive, toxic and flammable gases.

Therefore the preparation and the usage of new catalysts such as $K_2CO_3$ [12], $ZrO_2$ [13], $H_3PW_{12}O_4$–$ZrO_2$ [14], Cu modified (Ni, V, O) complex [15], $ZrO_2$–$CeO_2$ [16] were forced. The disadvantages such as the need of high pressure or the deactivation of the catalyst were also described and the reported formation rate of DMC was low. Various environmentally friendly chemical methods were developed like the transesterification of ethylene carbonate with methanol [17], and the synthesis from urea and methanol [18].

Carbonaceous materials have been used widely in catalysis because of their superior structural, mechanical, chemical, thermal, and unique electrical transport properties.

G. Merza · B. László · A. Oszkó · G. Pótári · E. Varga ·
A. Erdőhelyi (✉)
Institute of Physical Chemistry and Materials Science,
University of Szeged, Aradi vértanúk tere 1, Szeged 6720,
Hungary
e-mail: erdohelyi@chem.u-szeged.hu

Among the various catalysts CuCl$_2$/NaOH/activated carbon (AC) was reported to show good catalytic performance in the synthesis of DMC. The effect of reaction conditions and that of promoters on the reaction were evaluated [19]. The optimal reaction temperature was set to 393–403 K. The catalytic activity increased with the increase of OH/Cu molar ratio as compared to CuCl$_2$/AC. With the morphological analysis two different crystal structures were observed on the surface of the catalyst: orthorhombic and rhombohedral. The second one was more favourable for DMC synthesis [20].

Typical results were obtained on CuCl/Carbon in the oxidative carbonylation of methanol. It is clear that the CuCl$_3^{2-}$ surface species finally shifted to Cu$^0$ and cuprous chloride was identified as the active species in DMC production [21]. Ren et al. [22] observed that the activation temperature of the starch-based carbon supported Cu catalyst significantly influenced the activity of the sample, while the surface area, micropore volume and the total pore volume changed and these properties resulted in the different efficiency. The AC supported PdCl$_2$–CuCl$_2$ was also an efficient catalyst in this reaction but the activity of the sample significantly decreased in time. The results showed that the catalyst deactivation was due to the loss of chlorine [23].

Cu–Ni supported on multi-walled carbon nanotubes (MWCNT) was also used as catalyst for the direct synthesis of DMC connected with the full characterization of the sample. Relatively high methanol conversion and DMC selectivity were reported, though the optimal experimental conditions, like high pressure, have some inconveniences [24]. In a recent paper we discussed the yield of DMC formation which was higher on Cu/MWCNT than on Cu–Ni/MWCNT catalyst [25].

On a novel graphene nanosheet (GNS) Cu–Ni bimetallic catalyst the catalytically active metal particles were dispersed on the GNS in the direct synthesis of DMC and this effectively enhanced the productivity [26].

The mechanism of the oxidative carbonylation of methanol was theoretically investigated by Ren et al. The calculated results showed that the DMC formation pathway should be as follows: monomethyl carbonate (MMC) species produced by CO insertion to methoxide species, and then MMC reacts with methanol to form DMC [27].

Earlier AC (Norit) was successfully used as a catalyst support in different reactions. Solymosi et al. used Mo$_2$C/Norit in the decomposition and steam reforming of methanol [28], for the decomposition of ethanol [29], and also for the steam reforming and the decomposition of dimethyl ether (DME) [30]. Marbán et al. investigated Norit-supported Rh-based catalyst for the methanol decomposition reaction [31], Tolmacsov et al. tested Pt metals supported on Norit for the decomposition and reforming of methanol

[32]. Nevertheless we did not find any data in the literature about using carbon Norit as catalysts support operating in DMC synthesis.

In this paper we focus on the e synthesis of DMC at atmospheric pressure by vapour-phase oxidative carbonylation of methanol on copper supported by AC (Norit), a chloride free catalyst and on the catalytic properties during the reaction.

## 2 Experimental

### 2.1 Preparation of the Catalyst

Norit supported Cu, Cu–Ni and Ni catalysts were prepared via the conventional incipient wetness impregnation technique. The AC (Norit ROW 0.8 mm pellet from Alfa Aesar) was impregnated with Cu(NO$_3$)$_2$·3H$_2$O or/and Ni(NO$_3$)$_2$·6H$_2$O solution. In the bimetallic sample the Cu/Ni ratio was 2. In a typical preparation process calculated amount of the metal salt was dissolved in 25 % ammonia solution and then the support was added to yield 10 wt% metal content. The mixture was stirred for 24 h at room temperature followed by ultrasonication for 2 h, and aging for 24 h. The liquid was evaporated at 363 K. The dry powder was calcined at 723 K for 3 h in N$_2$ flow. The samples were reduced in situ usually at 873 K in hydrogen flow for 1 h. The BET surface area of the Cu/Norit was 1,070 m$^2$/g, of the Ni/Norit 900 m$^2$/g, of the Cu–Ni/Norit 951 and 1,212 m$^2$/g of the pure support.

The support was originally consisted of 0.8 mm o.d. and 3–4 mm long cylindrical pellets; this form was kept throughout the experiments. The average size of the metal particles was about 39 nm. Only 6 % of the Cu particles are smaller than 10 nm and about 20 % of them are bigger than 50 nm.

The metal clusters were roughly spherical on the surface of amorphous carbon.

### 2.2 Reaction Procedure

The DMC synthesis by the oxidative carbonylation of methanol was carried out in a continuous flow system in a fixed bed quartz reactor at atmospheric pressure. The reactor tube had an inner diameter of 7 mm with a length of circa 20 cm.

Methanol was introduced into the system by bubbling the mixture of CO and O$_2$ through the methanol at 323 K. Usually 1 g of the catalyst was used without dilution. After the pre-treatment of the sample the reactor was cooled down to the reaction temperature, usually 393 K. The ratio of the reactants (CH$_3$OH/CO/O$_2$ ratio was 2/1/1) was the same in all experiments. The flow rate was usually 16 ml/min.

The reactants and the products were analysed on-line by an Agilent 6890 gas chromatograph equipped with an Agilent 5975C VL MSD mass-spectrometer, thermal conductivity and flame ionization detectors.

## 2.3 Characterization of the Catalysts

For XPS studies the powder samples were pressed into tablets with approximately 10 mm diameter and a few tenth of mm thickness and placed into the load lock of the spectrometer. Sample treatments were carried out in a high pressure cell (catalysis chamber) directly attached to the analysing chamber and isolated from that with a gate valve. With the help of the sample manipulator and a second insertion mechanism it was possible to transfer the samples from the analysis chamber into the high pressure cell in vacuum, without the reach of air. The samples were pre-treated the same way as mentioned above. After each pre-treatment step the samples were cooled down in nitrogen flow to room temperature. Afterwards the flow was stopped, the high pressure cell was evacuated and the sample was taken back to the analysis chamber. XP spectra were taken with a SPECS instrument equipped with a PHOIBOS 150 MCD 9 hemispherical energy analyser operated in the FAT mode. The excitation source was the $K_\alpha$ radiation of a magnesium anode (h$\nu$ = 1,253.6 eV). The X-ray gun was operated at 210 W power (14 kV, 15 mA). The pass energy was set to 20 eV, the step size was 25 meV. Typically five scans were added to get a single spectrum. For data acquisition and evaluation both manufacturers' (Specslab2) and commercial (CasaXPS, Origin) software packages were used.

Infrared spectra were recorded with an Agilent Cary 670 type FTIR spectrometer equipped with diffuse reflectance attachment (Harrick) with $BaF_2$ windows with a wave number accuracy of $\pm 4$ cm$^{-1}$. Typically 32 scans were registered. The whole optical path was purged by $CO_2$- and $H_2O$-free air generated by a Balston purge gas generator. The catalysts were pre-treated as mentioned above then the $CH_3OH + CO + O_2$ mixture was introduced into the cell at the reaction temperature and the IR spectra were recorded. Practically the same experimental conditions were used as in the catalytic measurements.

The BET surface areas of the catalysts were measured using $N_2$ adsorption at the temperature of the liquid nitrogen by a BELCAT A instrument with single point method.

The Cu particle size distribution was determined by image analysis of the HRTEM (FEI Tecnai G$^2$ 20 X-Twin; 200 kV operation voltage, 180,000$\times$ magnification, 125 pm/pixel resolution) pictures using the ImageJ software. At least five representative images of equal magnification, taken at different spots of the TEM grid were first subjected to rolling ball background subtraction and contrast enhancement, and then the diameter of the metal nanoparticles in the image was manually measured against the calibrated TEM scale bar. Each diameter distribution histogram was constructed from 100 individual nanoparticle diameter measurements [33, 34].

## 3 Results and Discussion

### 3.1 Oxidative Carbonylation of Methanol

The catalytic reaction was intentionally performed at atmospheric pressure at 393 K, on Cu/Norit to obtain a 'greener' way for DMC synthesis. For comparison the tests were carried out also on Ni/Norit and on Cu–Ni/Norit catalysts.

In the reactions $CO_2$, DMC and methyl formate (MF) were formed as main products in all cases. A small amount of dimethoxy methane (DMM) and traces of DME were also detected. Figure 1a shows the conversion of methanol on Cu/Norit, which was increasing through the reaction, up to 22 % after 7 h time on stream. Figure 1b demonstrates that on Ni/Norit the methanol conversion was about 13 % at the beginning of the reaction, in the first 2 h it decreased continuously and after 150 min reached the quasi steady state value, about 2.5 %. The conversion of methanol on Cu–Ni/Norit increased up to 11 % in the first 130 min of the reaction attained a maximum and remained nearly the same (Fig. 1c). The CO conversion changed similarly to the methanol conversion in all cases. On the Ni/Norit it decreased in time but in the Cu containing samples the conversion increased as a function of time on stream (Fig. 1).

On Cu/Norit the formation rate of $CO_2$ in the first hour of the reaction increased, then decreased, after 3 h it remained nearly constant, while the formation rate of MF slightly increased in the first hour then remained the same (Fig. 2a). The formation of DMC started after the 100th min of the reaction evolved with an enhanced rate until the 350th min afterwards started to decrease. On Ni/Norit the rate of MF and $CO_2$ formation decreased in time, the DMC formation increased slightly at the same time although the production was less than measured on Cu/Norit (Fig. 2b). However, on Cu–Ni/Norit the rate of MF production significantly increased and that of $CO_2$ decreased slower in time, still the DMC and the DMM formation increased only a bit (Fig. 2c). It is clear from the above data, that under the same circumstances the rate of DMC formation was more than ten times higher on Cu/Norit as on Ni/Norit or on Cu–Ni/Norit after 5 h of the reaction.

The selectivity of MF remarkably increased at the beginning of the reaction on Cu/Norit. After reaching a

**Fig. 1** The conversion of CO
and methanol on Cu/Norit (**a**),
on Cu–Ni/Norit (**b**) and on Ni/
Norit (**c**) in the
$CH_3OH + CO + O_2$ (2:1:1)
reaction at 393 K, (The space
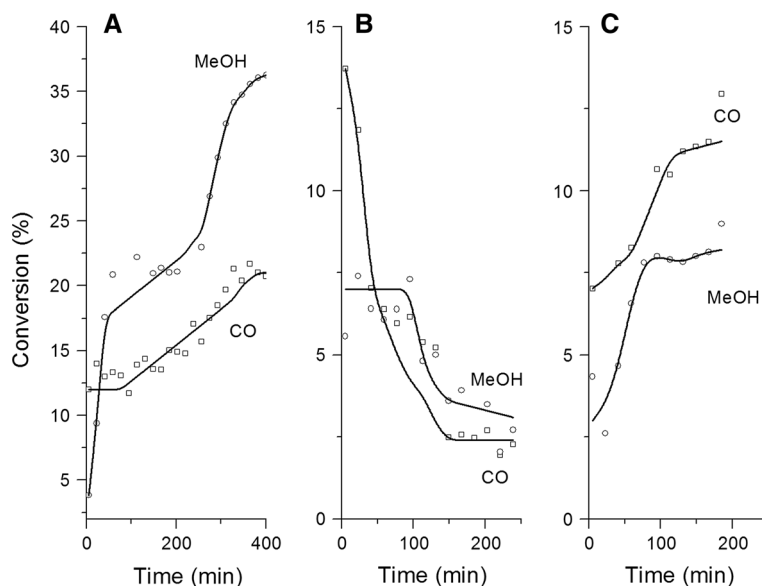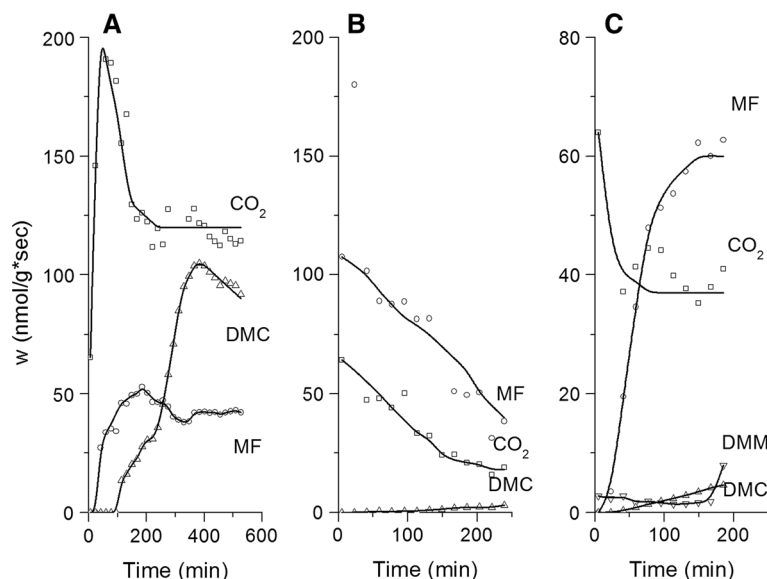velocity was 780 $h^{-1}$)



**Fig. 2** The rate of dimethyl
carbonate, methyl formate, $CO_2$
and dimethoxy methane
formation on Cu/Norit (**a**), on
Ni/Norit (**b**) and on Cu–Ni/
Norit (**c**) in the
$CH_3OH + CO + O_2$ (2:1:1)
reaction at 393 K, (The space
velocity was 780 $h^{-1}$)



maximum 33 % MF selectivity after 150 min it started to
decrease and stabilized after 300 min at 17 %. In the first
100 min of the reaction only traces of DMC was formed
then its selectivity increased gradually, after 300 min
stayed nearly constant, about 60 %. On the other hand,
$CO_2$ formation was the opposite, decreased drastically
from 100 % selectivity to 23 % after 300 min (Fig. 3a).

On Ni/Norit the MF (from 90 to 74 %) and the $CO_2$
(from 22 to 19 %) selectivity decreased (Fig. 3b). In the
first 100–120 min of the reaction only a small amount of
DMC was detected, afterwards with increasing selectivity
it reached only 10 % in the 250 min of the reaction. Fig-
ure 3c shows the selectivity of the products on Cu–Ni/
Norit. DMC selectivity marginally and that of MF notably

increased in the reaction, while the selectivity of $CO_2$
constantly decreased.

The yield of the DMC formation was the highest in the
steady state period at ambient pressure on Cu/Norit
($\sim$13.2 %) and it decreased in the order of Cu/Nor-
it > Cu–Ni/Norit > Ni/Norit. The value obtained on Cu/
Norit is comparable with the yield obtained on Cu/Y zeo-
lite (13.1 %) [35] or on CuCl$_2$ supported on AC (16.3 %)
[19] at 2.3 bar in an autoclave system, but it was definitely
higher than it was found on Cu–Ni/MWCNT at high
pressure [12] or on Cu/MWCNT at atmospheric pressure
[25].

When the catalyst was reduced at lower temperature (773
or 673 K) the induction time of DMC formation was

**Fig. 3** The selectivity of dimethyl carbonate, methyl formate, $CO_2$ and dimethoxy methane on Cu/Norit (**a**), on Ni/Norit (**b**) and on Cu–Ni/Norit (**c**) in the $CH_3OH + CO + O_2$ (2:1:1) reaction at 393 K, (The space velocity was 780 $h^{-1}$)
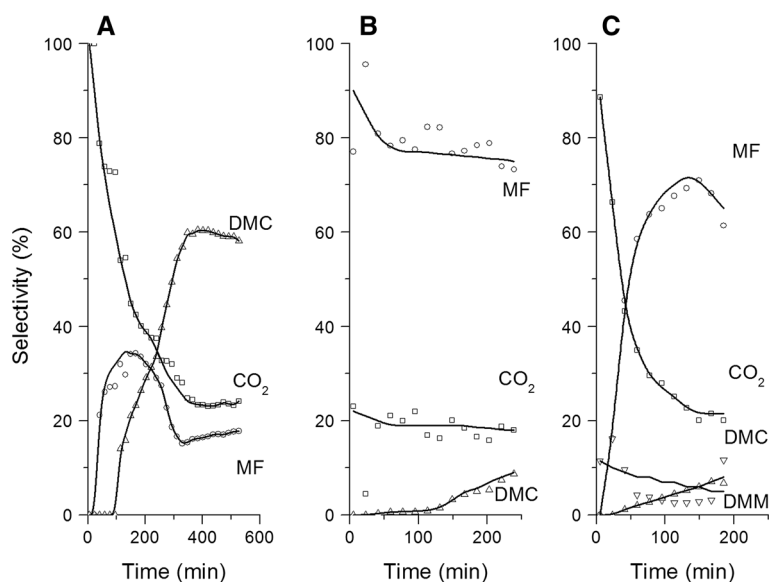


considerably longer (after the pre-treatment at 673 K it was 280 min), the DMC selectivity in the steady state was lower, below 20 % instead of 60 %. Without any pre-treatment the catalyst was totally inactive in the DMC synthesis.

When the methanol–oxygen reaction was followed under the same experimental conditions at 393 K, the methanol conversion was similar on either of the catalysts though in these cases MF was the main product, only a small amount of $CO_2$ and traces of formaldehyde were formed. The rate of products formation decreased in the first 30 min of the reaction then remained stable. In the methanol–CO reaction only $CO_2$ was formed.

The pure support was also used as catalyst in the same reaction using the same experimental conditions. In this case only a small amount of $CO_2$ was found as reaction product.

### 3.2 Catalytic Behaviour of Cu/Norit

The oxidative carbonylation of methanol was studied in detail on Cu/Norit. The reaction temperature was varied from 373 to 413 K. Each experiment was carried out on fresh catalyst. The steady state values obtained at different temperatures were compared. The rate of the products formation increased in all cases when the reaction was followed at higher temperature than 373 K. The amount of $CO_2$ increased continuously as a function of temperature but the MF and DMC formation curves had maxima at 383 and 393 K, respectively (Fig. 4a). It should be noted that the DMM formation rate significantly increased as a function of temperature; at 413 K it was about the quarter of the DMC production, while only traces were detected at 373 K. The selectivity of MF decreased by increasing the temperature, while that of DMC changed by giving a maximum curve.
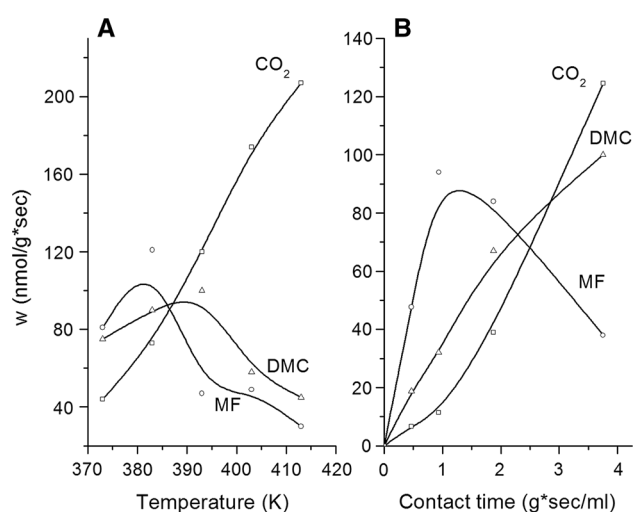


**Fig. 4** The formation rate of $CO_2$, dimethyl carbonate and methyl formate as a function of temperature (**a**) (contact time = 3.75 g sec/ml) and contact time (**b**) at 393 K in the $CH_3OH + CO + O_2$ (2:1:1) reaction on Cu/Norit approximately at the steady state conditions

The variation of the space velocity exerted divergent influence on the products distribution of the oxidative carbonylation of methanol. The conversion of methanol and the amount of DMC and $CO_2$ formed in the reaction increased quasi linearly with rising the contact time. In contrast the formation curve of MF had a maximum (Fig. 4b).

### 3.3 XP Spectra

In order to follow the changes of the surface composition and those of the oxidation states of the catalysts components XPS measurements were carried out during the catalytic reaction.

High-resolution XP spectra of Cu/Norit were taken in the Cu 2p, C 1s, O 1s and Cu LMM regions in all stages of the treatment. The Cu 2p doublet in the as received sample with Cu $2p_{3/2}$ at 933.6 eV showed the presence of $Cu(NO_3)_2$ [36] and CuO which probably formed in the decomposition of nitrate salt. Both the position of the Cu $2p_{3/2}$ peak and the presence of satellite features support this assertion. The peak location shifted to 932.4 eV after reduction at 873 K for 60 min and the satellites disappeared (Fig. 5). To distinguish between different copper oxidation states we must also take into account the Auger parameter, which in its simplified form of the sum of the binding energy of the Cu $2p_{3/2}$ photo peak and the kinetic energy of the $L_3MM$ Auger peak. This feature was located at 918.8 eV after reduction, thus giving 1,851.2 eV for the Auger parameter, so copper reduced to its metallic form and its surface concentration significantly increased during the reduction. In the course of the oxidative carbonylation of methanol the Cu $2p_{3/2}$ binding energy and the peak intensity did not change but the enhancement of a new peak around 944 eV (as a satellite) could be seen. This peak was observed even after 10 min of the reaction. After 60 min an intensifying shoulder could also be observed on the high binding energy side on both components of the Cu 2p doublet. The Auger spectra were more similar to the one taken in the as received state than to the spectrum taken after reduction. So we may conclude that copper was

oxidized in the reaction mixture and was mostly in the $Cu^+$ state, with some $Cu^{2+}$ also present on the surface. The amount of this latter species increased with increasing reaction time and was demonstrated by the intensifying satellite peak and shoulder on the copper spectra.

Similar spectra were obtained for the Cu component in the Cu–Ni/Norit catalyst. As regards the binding energy of Ni 2p in the as received sample the presence of NiO (855.6 eV) and a small amount of metallic Ni (852.7 eV) [37] were detected. The Ni 2p spectra of the reduced catalyst showed the presence of metallic Ni and $Ni^{2+}$ species at 852.7 and 855.6 eV, respectively. This indicates the existence of a fraction of unreduced Ni after the reduction of the sample in the Cu–Ni/Norit. On the Ni/Norit sample before the pre-treatment only the $Ni^{2+}$ was detected at 855.6 eV. On the reduced sample a new feature was also observed at 854.5 eV in addition to the metallic Ni (852.7 eV) which could be assigned also to $Ni^{2+}$ but in different chemical environment [38].

The survey spectra showed a very intense C 1s peak. High resolution carbon spectra taken on pure Norit and Cu/Norit featured a narrow asymmetric peak (FWHM = 1.3–1.4 eV) with a characteristic long tailing and shoulder on the high binding energy side (Fig. 6). On pure Norit an intense peak showed up at 284.5 eV in the as received state with components at $\sim$286–287, $\sim$290 and $\sim$293 eV. The 284.5 eV peak corresponds to C–C and



Fig. 5 XP spectra of Cu 2p (a) and Cu LMM Auger spectra (b) recorded after the $CH_3OH + CO + O_2$ reaction at 393 K on Cu/Norit; as received (1), reduced sample (2), after 10th (3), 60th (4) and 150th (5) minutes of the reaction
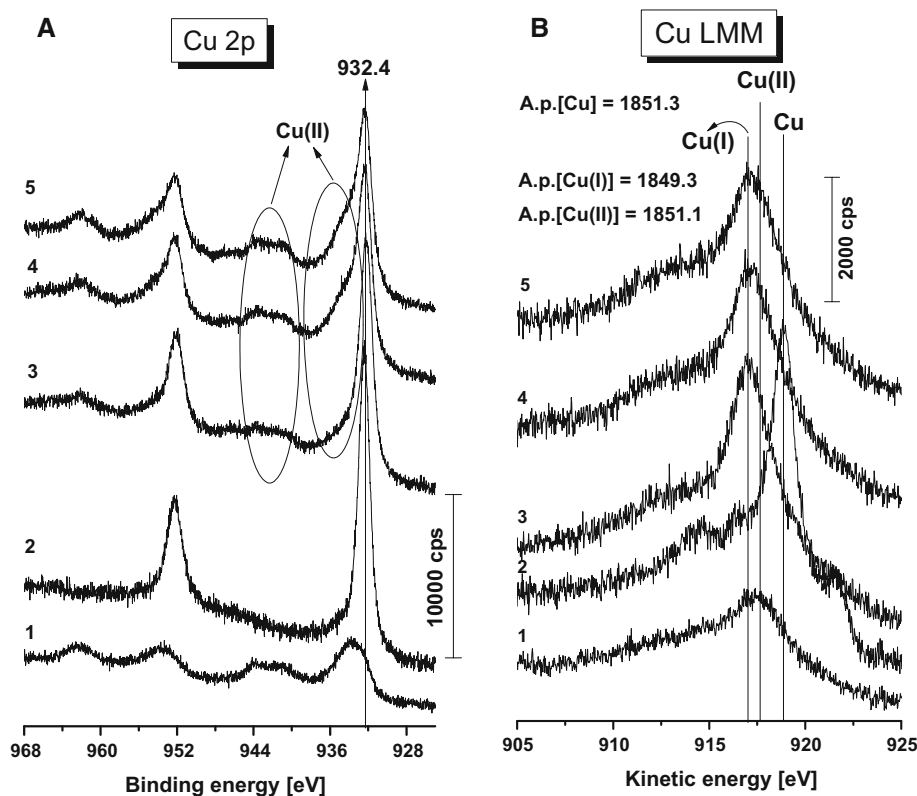
C–H bonds, while the 286 and 290 eV peaks to oxygenated carbon bonds like C–O (phenolic, alcoholic, etheric) and O–C=O (carboxyl, ester), respectively. The component with the highest binding energy may come from adsorbed CO or $CO_2$ or from the shake-up satellites from the π–π* transitions in aromatic rings [39, 40].

No changes were detected on pure Norit after a mild reduction with $H_2$ at 473 K for 30 min. The peak shape and peak areas remained practically constant throughout the experiment on the copper doped samples too; the change was well within 10 %. However the intensity of the component representing C–O groups markedly decreased. These also mean that we could not detect the formation of any new carbonaceous surface species during the reaction. The copper doublet is easily identifiable on the wide scan spectra but the O 1s region is hardly discernible, especially on the spectra of the treated samples. However high-resolution O 1s spectra showed that this region has a complex shape. In the O 1s region of pure Norit a peak located at 532.5 eV was detected with a shoulder at 537.4 eV. After reduction the intensity of the main peak reduced but its position did not change. The minor component shifted to 536.3 eV and its intensity increased relative to the main peak. The picture modified when spectra were recorded on Cu/Norit after reduction at 693 K for 60 min. In this case the O 1s spectrum could be fitted with four components, the most intense one being located at 533.2 eV (Fig. 7.). At the same time two minor shoulders could be identified at 536.6 and 530.6 eV. The peak fitting process required to suppose that an additional component is present peaking at 534.4.

After the oxidative carbonylation of methanol the line shape changed considerably, an intense peak developed around 530–531 eV even after 10 min time on stream but there was no change in the intensity during the reaction. The rendering of oxygen components is somewhat ambiguous in the literature. Some [39–41] assign the peak around 530–531 eV to oxygen in C=O bond, while Soria-Sánchez et al. put this component to 531.7 eV [42]. Since C=O bonds can occur in various groups at the edges of the carbon structure, both assumptions can be true. Electrons from copper–oxygen bonds can also contribute to this peak. Following the work of Figueiredo et al. [39] the peak at 533.2 after reduction can be attributed to –O– bonds. This peak vanished in the course of reaction, instead peaks developed at 532.7–532.9 eV, with increasing intensity during the reaction, characteristic of C=O bonds e.g. in anhydride. OH groups may also contribute to this feature. The peak at 534.0–534.4 eV may originate from carboxylic groups, while that at 536.1–536.6 eV was from adsorbed water. As already mentioned above, neither the intensity nor the shape of the C 1s spectrum changed remarkably during the reaction. Changes did occur in the structure of O 1s spectra however these are not reflected in the carbon line shapes. The reason for this was that after reduction on the sample the carbon to oxygen ratio at the surface was about 20:1. After 150 min of the reaction the oxygen content doubled to about 10 %, but this was still too few to cause major changes in the carbon spectra.

From the XP spectra the surface concentrations of metals on the pre-treated samples were also determined. On



**Fig. 6** XP spectra of C 1s recorded after the $CH_3OH + CO + O_2$ reaction at 393 K on Cu/Norit; as received (*1*), reduced sample (*2*), after 10th (*3*), 60th (*4*) and 150th (*5*) minutes of the reaction (**a**), the pure Norit (**b**)
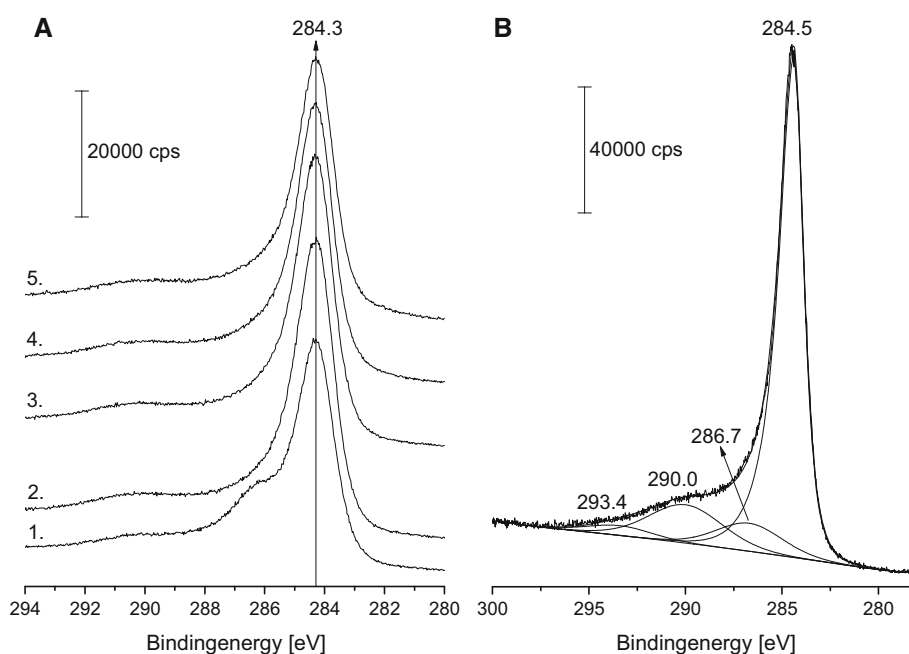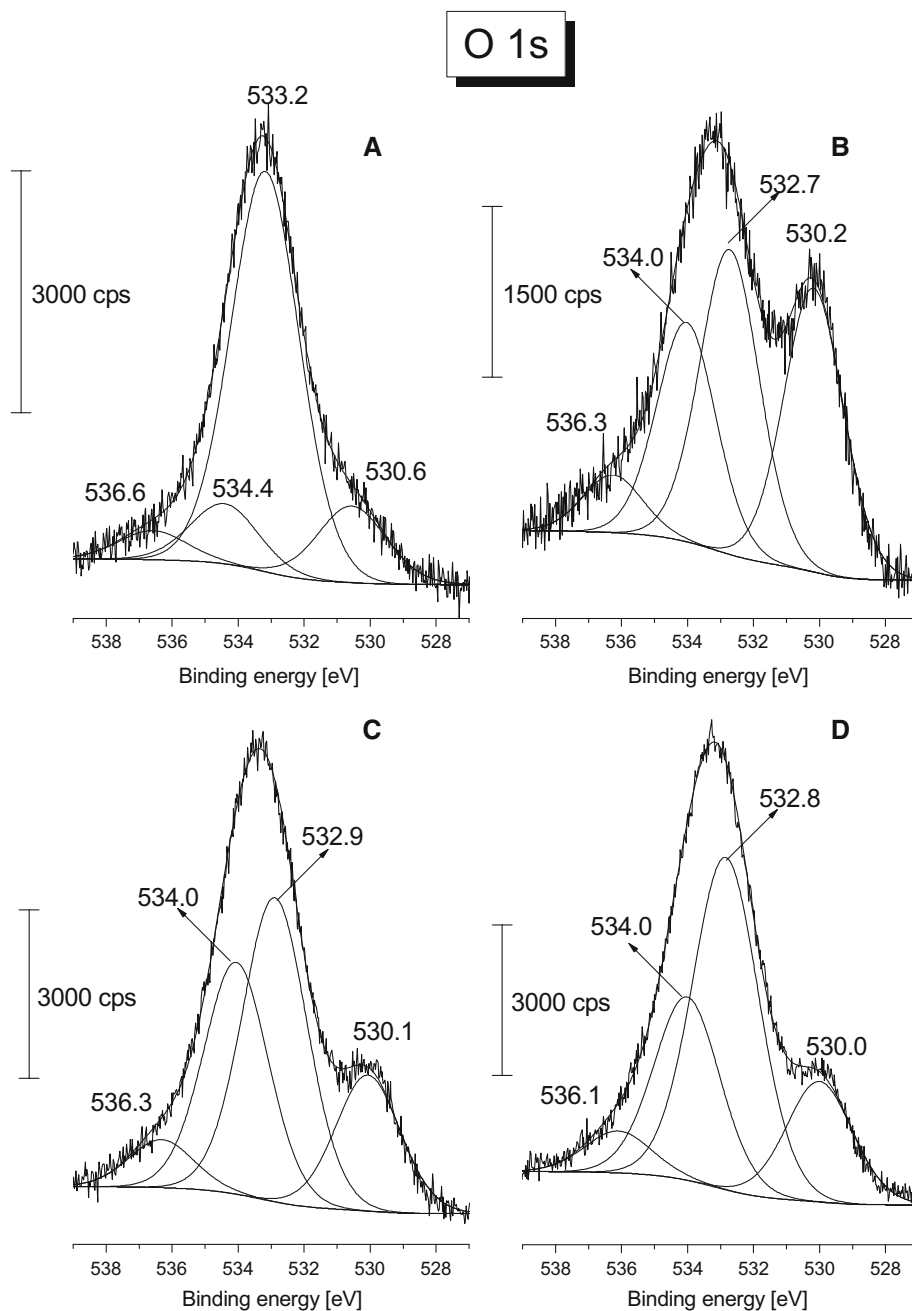
**Fig. 7** XP spectra of O 1s taken on Cu/Norit; reduced (**a**), after 10th (**b**), 50th (**c**) and 150th (**d**) minutes of the $CH_3OH + CO + O_2$ reaction at 393 K



reduced Cu/Norit the Cu content was 0.8 %, on Cu–Ni/Norit 2 % Cu and 4.8 % Ni was detected. On the surface of Ni/Norit the metal concentration was 6.2 %.

### 3.4 DRIFT Spectra Registered During the Reaction

The infrared spectra recorded in the DRIFT cell during the oxidative carbonylation of methanol on Cu/Norit at 393 K showed mainly the gas phase spectra of CO and methanol. If the spectra obtained on pure Norit under the same experimental conditions in the $2,200–1,000 \ cm^{-1}$ range is subtracted, absorptions at 2,141, 1,767, 1,610, 1,495, 1,404, 1,293–1,291, 1,066–1,053, 1,036–1,034 and 1,026–1,021 $cm^{-1}$ could be detected. The intensities of these bands changed in different ways during the reaction. The absorption at 2,141 $cm^{-1}$ diminuted, and the 1,767 and 1,292 $cm^{-1}$ features intensified in time. The intensity of the bands at 1,034 and 1,021 $cm^{-1}$ first evolved, but after 30 min of the reaction diminished (Fig. 8).

The bands at 2,141 $cm^{-1}$ are in the CO region. In contrast to earlier findings, the adsorption of CO on $Cu^{2+}$ or on metallic Cu sites were predominantly weak and

reversible at 300 K and above, still CO bonded most strongly on $Cu^+$ [43, 44]. London and Bell [45] found a sharp peak at 2,140 $cm^{-1}$ during the adsorption of CO on CuO, but Engeldinger et al. [39] observed the characteristic Cu(I)–CO band at 2,060–2,146 $cm^{-1}$ on Cu–Y depending upon the Cu content. Our XPS results demonstrated that $Cu^+$ and $Cu^{2+}$ also exist on the surface of the catalyst. Based on these results we cannot unambiguously assign this peak. The intensity of the absorption at 2,141 $cm^{-1}$ minimised in time during the reaction and according to the XPS results the amount of $Cu^{2+}$ grew on the surface, we may conclude that the CO absorbs at 2,141 $cm^{-1}$ and is bonded rather to $Cu^+$ than to $Cu^{2+}$.

In order to assignate the bands formed during the reaction below 2,000 $cm^{-1}$ we registered the infrared spectra of the main products on Cu/Norit catalyst. After the adsorption of DMC at room temperature bands were observed in the 2,000–1,100 $cm^{-1}$ region at 1,781, 1,768, 1,462, 1,454, 1,293 $cm^{-1}$. Similar spectra were recorded after the adsorption of DMC on multi-walled carbon nanotube supported Cu sample [25]. The bands at 1,781 and 1,768 $cm^{-1}$ could be attributed to $\nu$(C=O), those at 1,462 and 1,454 $cm^{-1}$ to $\delta_{as}$(–$CH_3$) in the *cis–trans* and *cis–cis* structure of DMC. The intensive absorption at 1,293 $cm^{-1}$ could be assigned to the $\nu_{as}$(O–C–O) vibration. Kar et al. [46] and Bohets and van der Veken [47] used a similar assignation for identifying the absorption bands obtained after DMC adsorption. In the 2,000 and 1,100 $cm^{-1}$ region in the spectra of MF adsorbed on Cu/Norit between peaks were detected at 1,768, 1,754 and 1,743 $cm^{-1}$ and a weak absorption was observed at 1,208 $cm^{-1}$. According to

Wilmhurst [48] the bands between 1,740 and 1,770 $cm^{-1}$ could be assigned as the C=O vibration of gas phase MF. Although both DMC and MF have absorption in this region, and an intense band was detected at 1,293–1,291 $cm^{-1}$ but when MF was adsorbed only a weak absorption was detected at 1,230 $cm^{-1}$ [48]. From these data we may suppose that the bands at 1,767 and 1,293–1,291 $cm^{-1}$ showed the presence of DMC on the surface of the catalyst.

The features at 1,459 and 1,404 $cm^{-1}$ detected at the beginning of the reaction are in the C–H deformation region and can be attributed to the anti-symmetric vibration of $CH_3$ and $CH_2$ groups of DMM, respectively [49].

The band at 1,610 $cm^{-1}$ is due to the adsorbed water formed in the reaction.

The interaction of $CH_3OH$ and Cu is summarised briefly for the assignation of the bands below 1,100 $cm^{-1}$. Previous studies demonstrated that methanol interacted weakly on clean Cu surface. It is necessary to activate the surface by partial oxidation; 20 % surface coverage by oxygen was required to achieve the maximum adsorption of methanol [50]. Methanol was found to adsorb dissociative on $Cu^+$ by the formation of methoxy species without additional supply of oxygen [44]. These findings demonstrate that the activation of methanol and CO occurs on the same sites, on $Cu^+$. The methanol adsorbed on $Cu_2O$ produces bands at 1,064 and 1,030 $cm^{-1}$ that was attributed to the C–O stretching and $CH_3$ rocking mode of methoxy, respectively [51]. According to these results the bonds observed at 1,068 an 1,036 $cm^{-1}$ could be assigned to the C–O stretching and CH rocking mode of methoxy

**Fig. 8** Infrared spectra registered during the $CH_3 + CO + O_2$ reaction at 393 K on Cu/Norit in the 10th (*1*), 20th (*2*), 30th (*3*), 90th (*4*) and 150th (*5*) minutes
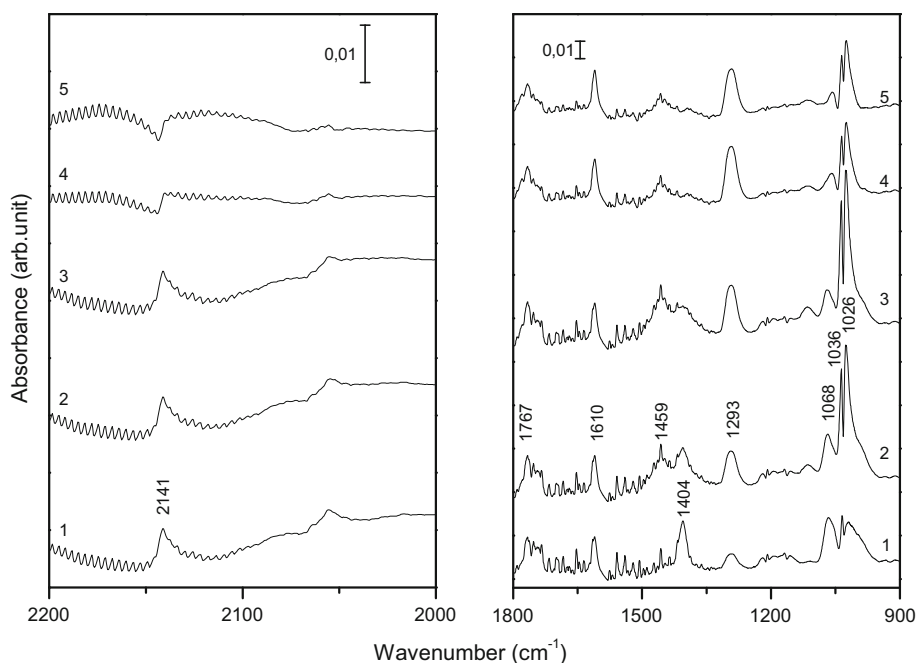
bonded to the oxidized Cu. Methoxy on Cu (100) surface reportedly absorb at 984 cm$^{-1}$ at 210 K [52], the C–O lies perpendicular to the surface. The band observed at 1,021–1,026 cm$^{-1}$ could be attributed to the C–O stretching vibration of CH$_3$–O bonded to another structure.

## 3.5 The Possible Route of DMC Formation

Cu/Norit showed remarkable catalytic properties in the oxidative carbonylation of methanol. The methanol conversion reached 22 % during the reaction, the CO conversion changed as the methanol conversion (Fig. 1a). The CO$_2$ formation rate first increased, then decreased, finally remained nearly constant. The MF formation rate after 100 min of the reaction remained quasi the same. The DMC formation started only after a 100 min induction period followed by a rapid formation until reaching the steady state (Fig. 2a).

XPS results showed that the reduced catalyst was oxidized in the reaction, thus the surface Cu was oxidized to Cu$^+$ and Cu$^{2+}$ (Fig. 5) and the amount of the latter species increased with increasing reaction time. The XPS studies of the pure Norit reveals that there was no significant change taking place on the surface of the support (Fig. 6) although the recorded O 1s spectra showed the change of the oxygen content of the catalyst (Fig. 7).

Infrared measurements revealed that the CO absorption is more favourable on Cu$^+$ than on Cu$^{2+}$ and that the activation of methanol is also occurring on Cu$^+$.

Earlier it was shown that Cu$^+$ ions are the active species in the DMC formation by oxidative carbonylation [6, 16]. A large number of experimental studies about the mechanism and kinetics of DMC formation on CuCl [3, 6, 16] or on Cu–zeolites [49] have been reported. DMC formation was stated to occur via two possible pathways. One of them is the CO addition to di-methoxide species, the other is the reaction of MMC and methanol to produce DMC [49].

In a theoretical investigation of the DMC formation on AC the reaction species were presented to be adsorbed on Cu$^0$/AC surface [27]. The calculated results indicated that DMC forms in the reaction of MMC with methanol.

Another theoretical analysis demonstrated that on Cu$_2$O(111) surface the CH$_3$O inhibit the CO adsorption together with the CO insertion to methoxide species for the production of MMC. Eventually the main reaction pathway is the reaction of these species with methoxy to form DMC [53].

The present paper supports a recent assumption in the literature for the DMC synthesis, namely that which emphasizes the strong connection with oxidized Cu as also demonstrated by the results of XPS studies (Fig. 5).

From the above mentioned DMC formation pathways our results verify a few statements, particularly where MMC species react with methanol. The MMC was stated to form by the CO insertion to the methoxy species however it was not found on the surface during the reaction. It could be explained by the high reactivity and low surface concentration. Still the dissociative adsorption of methanol on Cu$^+$ by the formation of methoxy species [44] and the strong CO adsorption to Cu$^+$ [43] were described in the literature.

Cu oxidization during the reaction was demonstrated by our XPS results (Fig. 5). First mainly Cu$^+$ species are formed on the surface, but later the amount of Cu$^{2+}$ increased in time. As it is illustrated by the DMC formation curve, when only metallic Cu is on the surface, in the first minutes of the reaction DMC was not produced. Later when only Cu$^+$ was detected on the catalyst DMC was also not detectable. By increasing the amount of Cu$^{2+}$ the DMC formation rate also increased but after some hours it slowly lessened (Fig. 3). The fully oxidized sample was totally inactive in the DMC synthesis. From these results we may conclude that both Cu$^+$ and Cu$^{2+}$ are necessary for the DMC synthesis, and in addition their ratio is decisive in the DMC formation. The changes of the oxidation state of Cu during the reaction could result in the changes of the DMC formation rate in time (Fig. 2) on Cu/Norit. Below is a proposed reaction pathway for DMC synthesis in which the following species
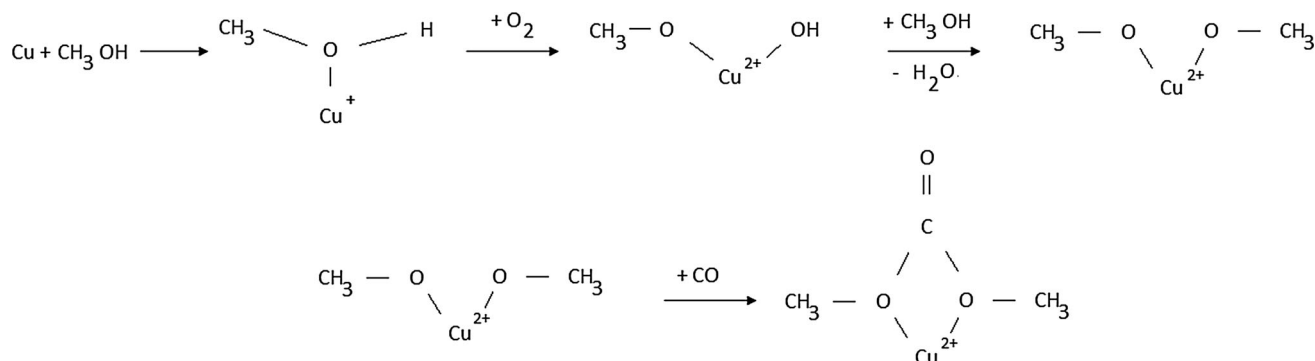
have an important role in the first two steps of the reaction. Insertion of CO into the latter species resulted in the DMC formation. Our XPS results support this theory, Zhang and Bell [49] suggested similar mechanism.

The results presented on Fig. 4b strongly suggest that the formation of MF occurs via another possible route. The O 1s signal of the catalysts indicates that the amount of carboxyl groups increased on the surface during the reaction so the direct interaction of the adsorbed methoxy species with the carboxyl groups could produce the MF.

Methanol adsorption on oxidized Cu on CuO surface results in the production of formate species [54] while either reacts with methanol and so MF is formed or decomposes to $CO_2$. These possibilities lead to the MF rate having a maximum as the function of temperature or contact time. The formation of MF and the decomposition or desorption of this product reduce the $Cu^{2+}$ centers which could reoxidize with oxygen.

## 4 Conclusion

In this work Cu, Ni and Cu–Ni/Norit catalysts were prepared, characterised, their catalytic activities were compared in the oxicarbonylation of methanol. Based on the experiments we can conclude the following:

Cu/Norit was a significantly effective catalyst for DMC synthesis. Under the optimal reaction conditions at atmospheric pressure the highest selectivity of DMC was about 60 % and the highest conversion of methanol was 22 % with the DMC yield of 13.2 % in the steady state of the reaction which is comparable with the previously reported ones at high pressure. The $CO_2$ formation rate was increasing with the temperature while MF and DMC formation rate changed through a maximum curve verifying that 393 K is the optimal temperature. The formation rate of DMC and $CO_2$ linearly enhanced by changing the contact time the formation rate of MF went through a maximum which is supposed to be the by-product of the reaction.

The XPS measurement results revealed that Cu/Norit catalyst went through changes. After reduction the catalyst was oxidized in the reaction, furthermore, the ratio of $Cu^+$ and $Cu^{2+}$ was determining in the DMC formation rate. The C 1s peak showed no significant change on the surface of the catalyst but from the O 1s spectra the change of the carbon and $O_2$ content was visible.

## References

1. Li C, Zhang X, Zhang S (2006) Chem Eng Res Des 87:1
2. Wen LB, Xin CY, Yang SC (2010) Appl Energ 87:115
3. Shivarkar AB, Gupte SP, Chaudhari RV (2005) J Mol Catal A 226:49
4. Ono Y (1997) Appl Catal A 155:133
5. Tharun J, Dharman MM, Hwang Y, Roshan R, Park MS, Park DW (2012) Appl Catal A 419:184
6. Li Z, Su K, Cheng B, Ming J, Zhang L, Xu Y (2011) Catal Commun 12:932
7. Litaiem Y, Dhahbi M (2012) J Mol Liq 169:54
8. Kim I, Ahn JT, Ha CS, Yang CS, Park I (2003) Polymer 44:3417
9. Seong P, Jeon BW, Lee M, Cho DH, Kim D, Jung KS, Kim SW, Han SO, Kim YH, Park C (2011) Enzyme Microb Technol 48:505
10. Giannoccaro P, Ravasio N, Aresta M (1993) J Organomet Chem 451:243
11. Keller N, Rebmann G, Keller V (2010) J Mol Catal A 317:1
12. Zhang B, Ding G, Zheng H, Zhu H (2014) Appl Catal B 152:226
13. Tomishige K, Sakaihori T, Ikeda Y, Fujimoto K (1999) Catal Lett 58:225
14. Jiang CJ, Guo YH, Wang CG, Hu CW, Wu Y, Wang EB (2003) Appl Catal A 256:203
15. Wang XJ, Xiao M, Wang SJ, Lu YX, Meng YZ (2007) J Mol Catal A 278:92
16. Tomishige K, Kunimori K (2002) Appl Catal A 237:103
17. Stoica G, Abelló S, Ramírez JP (2009) Appl Catal A 365:252
18. Sun J, Yang B, Wang X, Wang D, Lin H (2005) J Mol Catal A 239:82
19. Han MS, Lee BG, Suh I, Kim HS, Ahn BS, Hong SI (2001) J Mol Catal A 170:225
20. Han MS, Lee BG, Ahn BS, Kim HS, Moon DJ, Hong SI (2003) J Mol Catal A 203:137
21. Liu T, Chang CS (2007) J Chin Inst Chem Eng 38:29
22. Ren J, Guo C, Yang L, Li Z (2013) Chin J Catal 34:1734
23. Jiang R, Wang S, Zhao X, Wang Y, Zhang C (2003) Appl Catal A 238:131
24. Bian J, Xiao M, Wang S, Lu Y, Meng Y (2009) Appl Surf Sci 255:7188
25. Merza G, László B, Oszkó A, Pótári G, Baán K, Erdőhelyi A (2014) J Mol Catal A 393:117
26. Bian J, Wie XW, Wang L, Guan ZP (2011) Chin Chem Lett 22:57
27. Ren J, Wang W, Wang D, Zuo Z, Lin J, Li Z (2014) Appl Catal A 472:47
28. Barthos R, Solymosi F (2007) J Catal 249:289
29. Barthos R, Széchenyi A, Koós Á, Solymosi F (2007) Appl Catal A 327:95
30. Solymosi F, Barthos R, Kecskeméti A (2008) Appl Catal A 350:30
31. Marbán G, López A, López I, Solís TV (2010) Appl Catal B 99:257
32. Tolmacsov P, Gazsi A, Solymosi F (2009) Appl Catal A 362:58
33. Pótári G, Madarász D, Nagy L, László B, Sápi A, Oszkó A, Kukovecz Á, Erdőhelyi A, Kónya Z, Kiss J (2013) Langmuir 29:3061
34. Madarász D, Pótári G, Sápi A, László B, Csudai C, Oszkó A, Kukovecz Á, Erdőhelyi A, Kónya Z, Kiss J (2013) J Phys Chem Chem Phys 15:15917
35. Nam JK, Choi MJ, Cho DH, Suh JK, Kim SB (2013) J Mol Catal A 370:7
36. Wagner CD, Riggs WM, Davis LE, Moulder JF, Mullenberg GE (1992) Handbook of X-ray Photoelectron Spectroscopy, Perkin-Elmer, USA

37. Saw ET, Oemar U, Tan XR, Du Y, Borgna A, Hidajat K, Kawi S (2014) J Catal 314:32
38. Guczi L, Stefler G, Geszti O, Sajó I, Pászti Z, Tompos A, Schay Z (2010) Appl Catal A 375:236
39. Figueiredo JL, Pereira MFR, Freitas MMA, Órfão JJM (1999) Carbon 37:1379
40. Polovina M, Babic B, Kaluderovic B, Dekanski A (1997) Carbon 35:1047
41. Puziy AM, Poddubnaya OI, Socha RP, Gurgul J, Wisniewski M (2008) Carbon 46:2113
42. Sánchez MS, Valiente AM, Ruiz AG, Nevskaia DM (2010) J Colloid Interface Sci 343:194
43. Dandekar A, Vannice MA (1998) J Catal 178:621
44. Engeldinger J, Domke C, Richter M, Bentrup U (2010) Appl Catal A 382:303
45. London JW, Bell AT (1973) J Catal 31:32
46. Kar PB, Ramanathan N, Sundararajan K, Viswanathan KS (2012) J Mol Struct 1024:84
47. Bohets H, Veken BJ (1999) Phys Chem Chem Phys 1:1817
48. Wilmhurst JK (1957) J Mol Spectrosc 1:201
49. Zhang Y, Bell AT (2008) J Catal 255:153
50. Wachs IE, Madix RJ (1978) J Catal 53:208
51. Lin SD, Cheng H, Hsiao TC (2011) J Mol Catal A 342:35
52. Camplin JP, McCash EM (1996) Surf Sci 360:229
53. Zhang R, Song L, Wang B, Li Z (2012) J Comput Chem 33:1101
54. Poulston S, Rowbotham E, Stone P, Parlett P, Bowker M (1998) Catal Lett 52:63